Bridge Pile Response to Lateral Soil Movement Induced by Installation of Controlled Modulus Columns

Huu Hung Nguyen[1], Hadi Khabbaz[2], Behzad Fatahi[3], and Richard Kelly[4]

[1,2,3]*School of Civil and Environmental Engineering, University of Technology Sydney, Australia*
huuhung.nguyen@uts.edu.au, hadi.khabbaz@uts.edu.au, behzad.fatahi@uts.edu.au
[4]*SMEC Australia Pty Ltd, Australia, drrichard.kelly@smec.com*

Abstract

Controlled modulus columns (CMC) for ground improvement are installed using a hollow stem displacement auger to induce lateral soil displacement effect, followed by grout injection. While the method reduces spoils, the excessive lateral soil displacement may damage adjacent structures. Although there has been growing interest in quantifying such effects, only a handful of studies have been attempted. This paper presents the results of a numerical investigation on the CMC installation effect on an existing bridge pile using the three-dimensional finite difference software package $FLAC^{3D}$. It has been found that when the CMC is long and the existing bridge pile is slender, the pile bending moment and pile lateral movement, induced by the CMC installation effect, can be significant.

Keywords: ground improvement, controlled modulus columns, installation effect, cavity expansion, bridge pile

1 Introduction

The controlled modulus column (CMC) ground improvement technique aims to create an improved composite ground, consisting of a grid of rigid inclusions installed in soft soil overlaid with a granular load transfer layer (Plomteux et al. 2004). The column installation process involves penetrating an auger into the ground under a torque and thrust provided by a drilling rig, followed by grout injection through the hollow stem while raising the tool. The auger is purposely designed to enable lateral soil compaction during augering and prevent the soils from moving upward when raising the auger. When construction sites involving CMC are located in close proximity of existing sensitive structures such as an existing bridge foundation, if proper installation sequence is not considered, the risk of damaging adjacent structures due to lateral soil movement can be high (Plomteux et al. 2004, Brown 2005, and Hewitt et al. 2009). Hence, it is often necessary to prepare a risk assessment and construction planning before construction starts. Although these tasks have become a routine for piling contractors, assessing installation effects, especially the lateral soil

movement due to installation, remains a serious challenge. Available assessment methods for installation effects include the cavity expansion theory (Carter et al. 1979), strain path method (Baligh 1985) and more rigorous analyses using numerical modelling. The cavity expansion theory, which is the most common method, studies the changes in pore water pressure and stresses due to the creation or the expansion of a cavity. Current contributions to CMC application found in the literature include a numerical study by Rivera et al. (2014) based on the cavity expansion theory using PLAXIS-2D and a field investigation of installation effects on the surrounding soils by Suleiman et al. (2015). However, assessment of the CMC installation effects on the adjacent existing structures has not been reported in the literature notably due to a number of reasons. Firstly, the modelling of pile installation process involves large mesh distortion and can be time consuming. Secondly, the existing analytical methods are unable to capture the complex three-dimensional soil-structure interaction and construction sequence. This paper presents a 3D numerical model to investigate the response of an existing bridge pile subjected to loading due to the lateral soil movement induced by the installation of nearby CMCs.

2   Numerical Modelling

To simulate the CMC installation process, three dimensional numerical modelling using $FLAC^{3D}$ v.5.01 was carried out in large strain mode. 3D grids were created to represent a soil profile consisting of a soft clay layer, overlying bedrock (Figure 1a). An existing bridge pile and six proposed CMC positions are located in the centre of the 3D model. The radial cylindrical mesh represents CMCs and piles, while the cubical meshes form the outer soil regions. The lateral boundaries were extended 20 times the CMC diameter, from the outmost CMC or pile to minimize the boundary effects.
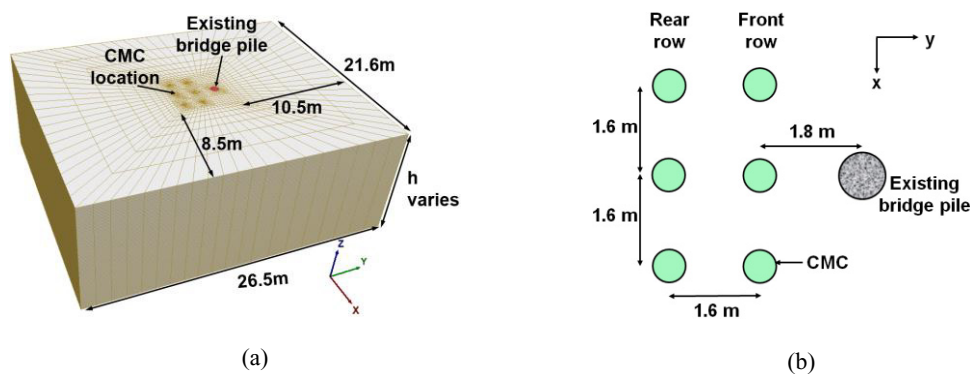

Figure 1: (a) $FLAC^{3D}$ finite difference grid and (b) the layout of CMCs and the existing bridge pile

The existing bridge pile is 0.75 m in diameter (d) and is located at 1.8 m centre to centre (c/c) from the nearest CMC. The pile is assumed socketed into the bedrock. The construction of two rows of CMCs next to the existing bridge pile was simulated in this study (Figure 1b). Each row has three columns oriented in the x-direction. CMCs have a diameter d_{CMC} = 225 mm and spaced at 1.6 m c/c in a square pattern. All CMCs are installed to the top of bedrock or very stiff ground. The model grid is generated using *FISH* programming language to facilitate the parametric studies. The 3D grid shown in Figure 1a developed for a model height h = 9.6 m comprises 179,200 zones and 165,616 grid points.

2.1   Material Model

Soil properties were derived from site investigation data from a highway upgrade project in Australia. The modified Cam-Clay (MCC) material model was adopted to represent the behaviour of the soft clay. The adopted parameters include the slope of normal consolidation line (NCL) λ = 0.29,

and the slope of elastic swelling line κ = 0.073. The NCL line is defined by a reference pressure p'_{ref} = 74 kPa and a specific volume v_{ref} = 2.55. Based on the oedometer results, an overconsolidation ratio OCR of 1.6 was adopted for the entire depth. Therefore, the pre-consolidation pressure varies linearly with depth. The adopted effective friction angle ϕ' is 28° and the frictional constant of the critical state line is M = 1.11. The lateral stress coefficient K_0 for lightly overconsolidated clay can be related to that of the normally consolidated clay via OCR and was estimated to be 0.75 (i.e. simulating anisotropic stress conditions). Other typical properties for soft clay including a dry density of 1300 kg/m^3, a porosity of 0.5 and an effective Poisson's ratio v' = 0.3 were also adopted. It is noted that for a structured clayey soil, due to increase in the mean effective stress as well as deviatoric stress, cementation degradation may occur influencing the deformation of the ground immediately after the installation (Nguyen et al. 2014).

Both pile and CMC are considered impermeable and modelled using solid elements. The pile is characterized by an isotropic linear elastic model, described by a Young's modulus of 20 GPa, a Poisson's ratio of 0.2 and a density of 2400 kg/m^3. The Mohr Coulomb (MC) material model was used to represent CMC behaviour. In this study it was assumed that the CMC grout set quickly after injection. Hence, a grout density of 2400 kg/m^3, bulk modulus K = 3.23 GPa, shear modulus G = 2.42 GPa, the cohesion c' = 300 kPa, the friction angle ϕ'= 5°, and a tensile strength σ^t = 520 kPa were adopted for CMC simulation. The stiffness and the tensile strength of CMCs were estimated according to Eurocode 2 (BSI 2004) using a characteristic compressive strength of sand concrete f_{ck} = 10 MPa.

2.2   Interfaces, Boundary and Initial Conditions

To allow gapping or sliding between the soft clay and CMC/pile, interface elements with insignificant tensile strength were employed. The interface behaviour is determined by the friction angle and cohesion, which were set equal to those of the soft clay. The interface normal and shear stiffnesses are estimated using Equation 1 as recommended by Itasca (2012).

$$k_n = \ k_s \ \approx \ 10 \times \left[\frac{K + \frac{4}{3}G}{\Delta z_{min}} \right] \tag{1}$$

where K and G are the maximum values of bulk and shear moduli of the soil, respectively; and Δz_{min} is the minimum mesh size in the elements adjacent to the interface.

The soil at the side boundaries in Figure 1a is fixed against the displacement normal to the boundary planes. The top boundary is free and is considered permeable (free draining). The bottom boundary is restrained vertically, for the purpose of radial cavity expansion. The initial conditions include the initial hydrostatic pore water pressure assuming groundwater table at the ground surface; and initial effective stresses due to soil self-weight, assuming a gravitational acceleration of 9.81 m/s^2. However, near surface soils in reality may be partially saturated and a more realistic coupled flow-deformation behaviour of unsaturated soils should be considered (Ho et al. 2015). Once the in-situ stresses are established, the bridge pile is installed by simply changing material properties in the pile zones, from those of soil to concrete and the system is stepped to equilibrium.

2.3   Modelling CMC Installation

The simulation of the CMC installation process is executed in two stages: (i) creating a cylindrical borehole and (ii) backfilling the borehole with CMC grout.

Cavity creation is most easily modelled numerically by expanding a pre-existing cavity of initial radius r_i to a new cavity of radius r_f, as recommended by Carter et al. (1979). Assuming undrained expansion, the condition of constant volume can be considered and hence, the radius r_f at end of the

expansion can readily be estimated using a simple relationship: $r_f = (r_i^2 + r_{CMC}^2)^{0.5}$ where $r_{CMC} = 225$ mm. An optimal initial radius r_i was determined, being sufficiently small to maintain reasonable numerical accuracy. At the same time, this radius should not be too small, to avoid excessive mesh distortion. Parametric studies indicate that $r_i = 65$ mm (i.e. approximately $\frac{1}{4}$ of r_{CMC}) is adequate for the adopted geometry and mesh. The first step of creating a cavity was to turn the soil within the initial cavity of $r_i = 65$ mm into "null" material (i.e. material removed). In the next step, outward normal velocities were applied to the cavity wall so that, upon mechanical stepping in a large strain mode, the wall displaced in the radial direction until achieving the final cavity radius of 234 mm. It is noted that, during expansion, the tangential velocity at the wall was fixed to zero. The deformed mesh as a result of cavity creation at the first CMC is shown in Figure 2.

Before filling the borehole with the CMC grout, the applied velocities at the cavity wall were removed and the model is stepped to equilibrium. Following grouting, the base of the newly formed CMC was restrained vertically. The soil/CMC interface elements were inserted and the system was then stepped to equilibrium to complete the CMC installation. The subsequent CMC installations were simulated in a similar manner, according to a sequence shown in Figure 3, i.e. starting with the rear row (CMCs 1 to 3) and then progressing to the front row (CMCs 4 to 6).
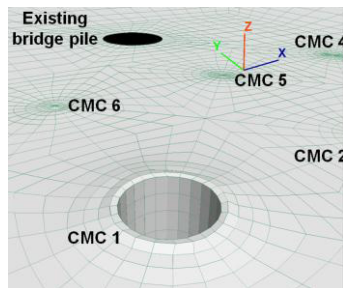

Figure 2: Deformed mesh after undrained cavity creation at the first CMC
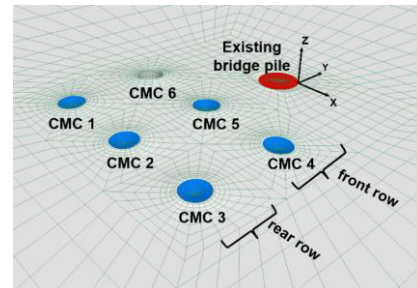
Figure 3: The order of CMC installation

3 Results and Discussions

Soil movement due to CMC installation is verified against a number of assessment methods published in the literature, firstly, under plane strain condition: (i) analytical closed-form undrained cavity creation solution (i.e. expansion from $r_i = 0$), suggested by Carter et al. (1980) for pile driving (ii) recommended numerical procedure by Carter et al. (1979) and (iii) $FLAC^{3D}$ with varying initial cavity radii (Figure 4). It is found that numerical analyses with the currently adopted $r_i = 65$ mm or so yield soil movement somewhere between the closed-form solution ($r_i = 0$) and the numerical results suggested by Carter et al. (1979) ($r_i = 130$ mm). Hence, the soil movement is much dependent on the chosen r_i. In addition, the soil movement at various depths of the 3D model is compared with the plane strain solution (Figure 5). At the ground surface, with much heave occurring, the estimated radial soil movement is the least. The radial soil movement at larger depths is greater, but less than the soil movement numerically analysed under plane strain condition.

Figures 6 to 9 present the results of the numerical simulation of CMC installations in a soft clay layer extending to a depth of 9.6 m below the ground surface, with pile length $L = 9.6$ m. In particular, Figure 6 shows that during installation the pile head moves away from the CMCs as expected. However, the pile head also moves slightly sideway, i.e. in the negative x direction. It is noted that the direction of pile head movement can be different if the installation sequence differs from that

described in Figure 3. The side-way movement of pile head in the x direction is the consequence of the change in the direction of the lateral soil movement induced by the installation of different CMCs.
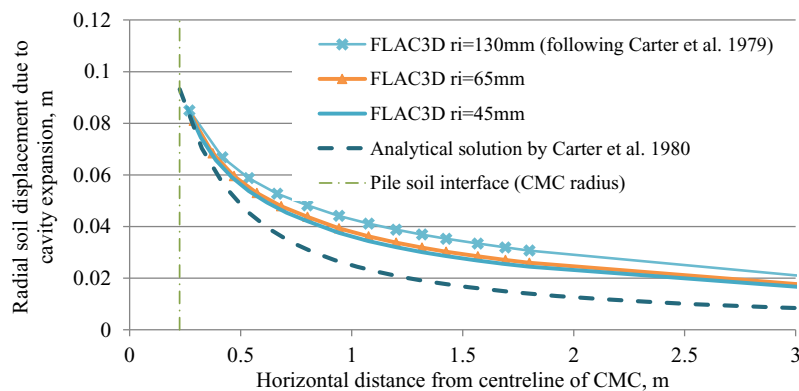

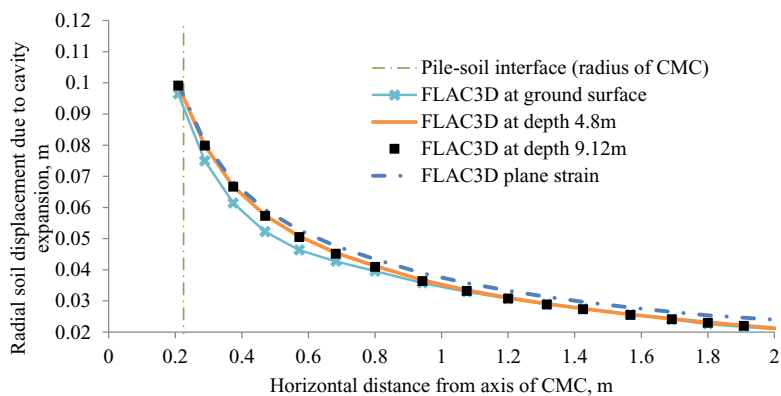**Figure 4**: Radial soil movement due cavity expansion versus horizontal distance from CMC axis

Figure 5: Radial soil displacement versus horizontal distance from CMC axis by depths

Figure 7 presents a cross section through the pile centre together with the contour of the excess pore water pressure at the completion of all CMC installations. It is clearly observed that the pore water pressures increase significantly in front of the pile along line A-B, while the pore water pressure values behind the pile are less than the initial hydrostatic pore pressures, due to the decompression of the soil. Figure 8a illustrates the excess pore water pressure in front of the pile (i.e. along line A-B shown in Figure 7), due to the undrained cavity expansion. The excess pore water pressure due to the installation of the rear row is relatively small; however, a substantial increase in excess pore water pressure occurs when the front row CMCs are installed. The installation of CMC 5, which is the closest CMC to the bridge pile, causes the most significant excess pore water pressure increase. The excess pore pressure is expected to decay inducing elastic visco plastic deformation (Le et al. 2015). The normal stresses acting on the pile shaft presented in Figure 8b indicate a similar pattern to the pore water pressure reported in Figure 8a.

The response of the existing bridge pile foundation to the lateral soil movement induced by the CMC installation process was recorded in terms of lateral deflection in the y direction (Figure 9a) and the induced bending moment (Figure 9b). As expected, the lateral deflection increases as more CMCs are installed, with much greater effect due to the front row than the rear row. A maximum pile lateral deflection of approximately 49 mm occurs at the top of the bridge pile. According to Stewart et al. (1994), horizontal displacement of less than 25 mm is often considered to be acceptable and

movements greater than 50 mm are generally unacceptable. When the pile is longer and hence more slender, the pile movement may be more significant. The calculated maximum bending moment in the pile is approximately 1,140 kNm, which occurs at the bottom of the bridge pile. In this study, the soil is homogenous with the soil undrained shear strength increasing linearly with depth, resulting in a straightforward prediction of the maximum bending moment location. It should be noted that for a stratified soil profile, the location of the maximum bending moment may be positioned elsewhere. In addition, it is noted that the head restraint is not provided to the existing pile. According to Poulos (1994), the existence of restraint at the pile head may lead to bending moments that are two or more times the value for an unrestrained pile head.
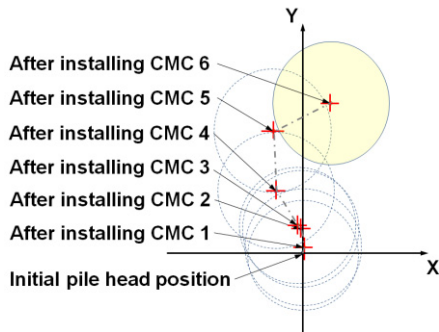

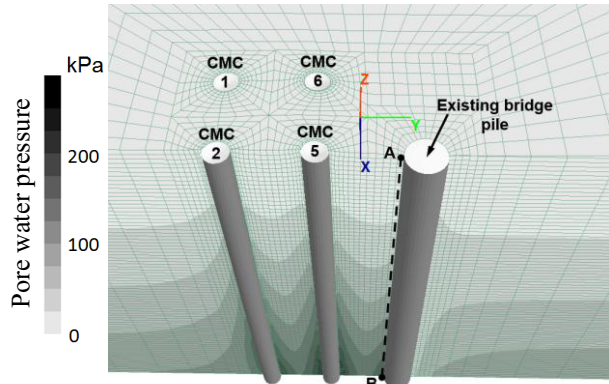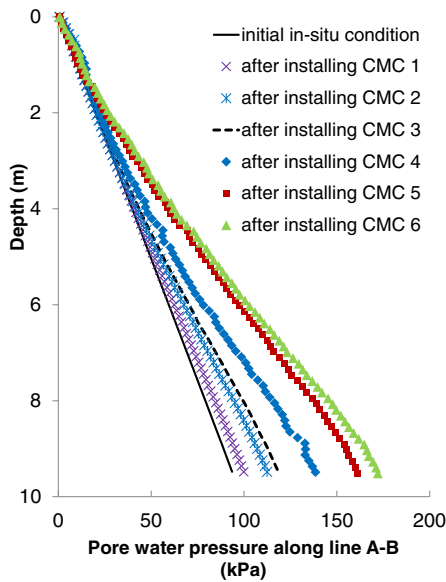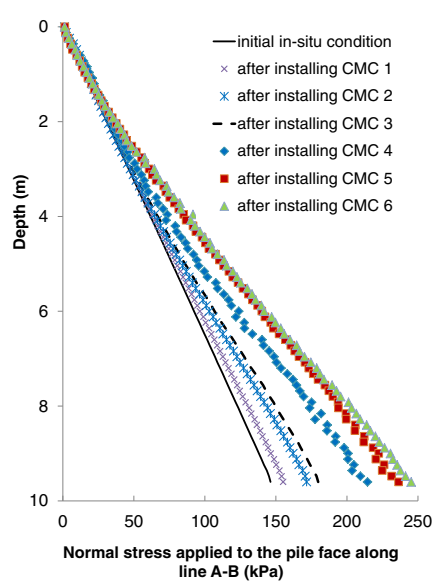**Figure 6:** Pile head movement during CMC installation process (L_{pile} = 9.6m)

Figure 7: Pore water pressure upon complete installation of the final CMC

(a)   (b)

Figure 8: (a) Pore water pressure near pile face (b) Normal stress acting on the pile face after CMC installation

A parametric study was carried out to quantify the effect of varying the soft soil thickness, hence the lengths of the CMCs and bridge pile, on the CMC installation effect on the behaviour of the bridge

pile. Therefore, two more sets of analyses were carried out, with the adopted soil thicknesses of 4.8 m and 7.2 m, in addition to the previous set of analysis corresponding to the soil thickness of 9.6 m. A single bridge pile diameter is adopted for all analyses; hence the pile slenderness increases with the increase in the pile length (or the soil thicknesses). The results shown in Figures 10a and 10b indicate that for pile lengths of 4.8 m, 7.2 m and 9.6 m, the pile head lateral movements are 4 mm, 23 mm and 49 mm; and the corresponding pile bending moments are 275 kNm, 740 kNm and 1,140 kNm, respectively.
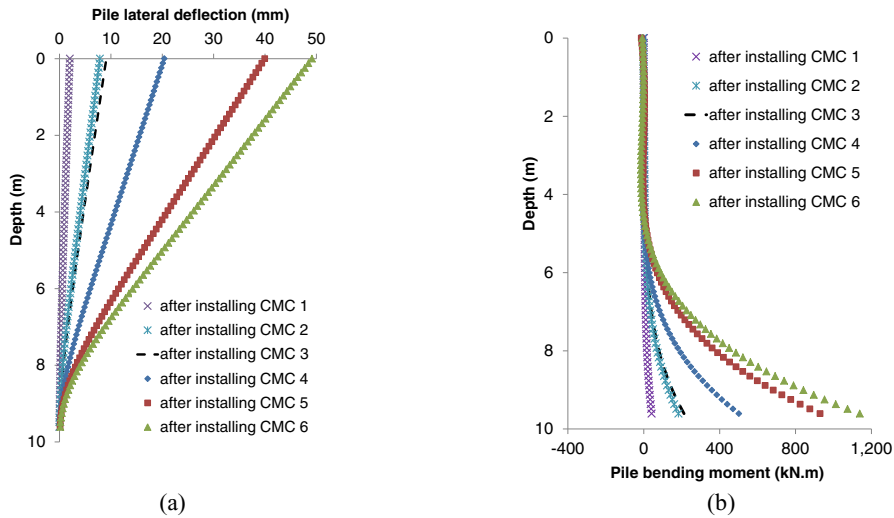

(a)   (b)

Figure 9: Bridge pile response: (a) lateral deflection and (b) bending moment

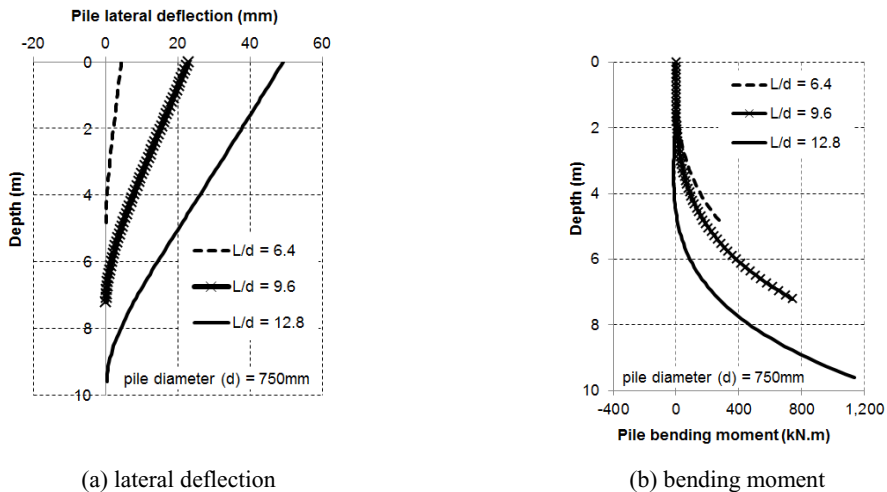(a) lateral deflection   (b) bending moment

Figure 10: Bridge pile response upon complete installation of the final CMC for three model depths

The results indicate that the soft soil thicknesses and the CMCs' length have significant effects on the bridge pile response to the lateral soil movement induced by the CMC installation. Thus, any realistic assessment of CMC installation effects on the existing surrounding structures, particularly piles, should include detailed considerations of CMCs, piles and soft soil properties.

4   Conclusions

The installation process of controlled modulus columns (CMC) in soft soil has been simulated using $FLAC^{3D}$ to investigate the short term effect on an existing bridge pile. The results indicate the feasibility of simulating the installation process numerically. The numerical results shows that undrained excess pore water pressure in front of the bridge pile and the normal stress applied on the bridge pile increase as more CMCs are installed. As the CMCs are longer and the bridge pile is more slender, the lateral pile deflection increases. The results indicated that the lateral pile deflection due to the horizontal soil movement induced by the CMC installation can be significant; hence, it highlights the importance of accurate assessment of CMC installation effect on the surrounding structures prior to construction, in addition to traditional observation methods commonly adopted during construction.

References

Baligh, M. M. (1985). "Strain path method." *Journal of Geotechnical Eng.*, Vol. 111(9): 1108-1136.

Brown, D. A. (2005). Practical considerations in the selection and use of continuous flight auger and drilled displacement piles. *ASCE - Geotechnical Special Publication No 132*, Texas, US.

Carter, J. P., Randolph, M. F. and Wroth, C. P. (1979). "Stress and pore pressure changes in clay during and after the expansion of a cylindrical cavity." *Int. J. for Numerical and Analytical Methods in Geomechanics*, Vol. 3(4): 305-322.

Carter, J. P., Randolph, M. F. and Wroth, C. P. (1980). Some aspects of the performance of open- and closedended piles. Numerical methods in offshore piling: pp 165-170.

Hewitt, P., Summerell, S. J. and Huang, Y. (2009). Bridge approach treatment works on the coopernook to herons creek section of the pacific highway upgrade. *Geosynthetics: New materials for modern infrastructure, Australian Geomechanics Society*.

Ho, L., Fatahi, B. and Khabbaz, H. (2015). "A closed form analytical solution for two-dimensional plane strain consolidation of unsaturated soil stratum." *Int. J. for Num. and Anal. Methods in Geomechanics*, Vol. 39(15): 1665-1692.

Itasca (2012). Flac3d - fast lagrangian analysis of continua in 3 dimensions, version 5.01. Minneapolis, Itasca Consulting Group, Incorporated.

Le, T. M., Fatahi, B. and Khabbaz, H. (2015). "Numerical optimisation to obtain elastic viscoplastic model parameters for soft clay." *International Journal of Plasticity*, Vol. 65: 1-21.

Nguyen, L. D., Fatahi, B. and Khabbaz, H. (2014). "A constitutive model for cemented clays capturing cementation degradation." *International Journal of Plasticity*, Vol. 56(0): 1-18.

Plomteux, C., Porbaha, A. and Spaulding, C. (2004). Cmc foundation system for embankment support—a case history. *GeoSupport 2004: Drilled Shafts, Micropiling, Deep Mixing, Remedial Methods, & Specialty Found. Sys.*, ASCE.

Poulos, H. (1994). "Effect of pile driving on adjacent piles in clay." *Can. Geot J.*, Vol. 31(6): 856-867.

Rivera, A. J., et al. (2014). Numerical modeling of controlled modulus column installation in soft soils using a linear elastic perfectly plastic soil model. *8th European Conf n Num. Methods in Geot.Eng.*, The Netherlands, CRC Press.

Stewart, D. P., Jewell, R. J. and Randolph, M. (1994). "Design of piled bridge abutments on soft clay for loading from lateral soil movements." *Geotechnique*, Vol. 44(2): 277-296.

Suleiman, M., et al. (2015). "Installation effects of controlled modulus column ground improvement piles on surrounding soil." *J.of Geot.and Geoenv Eng.*, Vol. 142(1): 04015059.